3rd National Conference on Petroleum Geomechanics
National Iranian Oil Company Exploration Directorate
Tehran, Jan,22-23,2019

Prediction of Volume and Rate of Sand Production Using a Hydro-mechanical Sand Erosion Model

Majid Fetrati[1]; Ali Pak[2]

ABSTRACT

Sand production is an unfavorable issue that occurs during extraction of oil from sandstone reservoirs. Several parameters affect sand production, including mechanical failure of materials around the wellbore, material erosion due to fluid flow, flow rate and type of perforations. The coupling between mechanical failure and hydrodynamic erosion of the rock is the key issue in analyzing sand production problem. This paper examines the applicability of a coupled hydromechanical and erosion criterion for simulating sand production using the finite element method. For this purpose, Abaqus software is used for numerical modeling, and the porous medium is considered fully saturated. The problem can be simulated in 2D or 3D (axisymmetrical). Sanding model that used in this study predicts the onset of sanding and volumetric production of sand with coupling between mechanical failure and subsequent erosion of the solid particles due to fluid flow. For simulating erosion, a number of sand erosion criteria proposed by various researchers implemented into the finite element code. Erosion equations are defined using specific subroutine written in Fortran and linked to Abaqus. Arbitrary Lagrangian-Eulerian (ALE) adaptive mesh technique was used in the domain near the wellbore. Also, the Map solution technique was used in order to eliminate the problem of mesh distortion. Sand production in the horizontal wellbore and perforated casing was simulated to demonstrate capabilities of the proposed model. The obtained results indicate the efficiency of the model used in the evaluation of sanding in sandstone reservoirs.

Keywords: Sand production, Numerical modeling, Finite element method, Sanding criteria, Erosion model.

1. INTRODUCTION

One of the most challenging issues in the oil industry is sanding phenomenon in the extraction wellbores. When hydrocarbons are produced from a sandstone reservoir, under special circumstances, sand particles move from the reservoir into the well along with the hydrocarbon flow. This unintended byproduct of the hydrocarbon production is called “sand production” [1]. Sand production imposes adverse impacts on the production cost as gas and oil industries have faced for decades. Corrosion of the pipelines, surface facility deterioration, sand-oil separation cost, and casing collapse are some of the problems pertaining to sand production [2].

There are different methods for modeling the sand production phenomenon such as FDM, FEM, and DEM. Discontinuum approach is promising to simulate phenomena such as detachment of individual particles from the rock matrix which is a useful tool to understand the mechanism of sanding [3]. However, there are some limitations to this approach. Not only does the discontinuum approach need considerable computational effort comparing to the

[1]Corresponding Author: Graduate Student, Department of Civil Engineering, Sharif University of Technology, fetrati.majid1993@gmail.com

[2]Professor, Department of Civil Engineering, Sharif University of Technology, pak@sharif.edu

continuum approach, but it also has serious limitations for simulating real scale problems. Thus it can be applied merely for small-scale problems.

Sand production phenomenon has been investigated and discussed for decades. Detournay [4], Pak et al. [5], Nouri et al. [6], and Bodaghabadi et al. [7] predicted the amount of sand production using FDM method. Li et al. [8], Eshiet and Sheng [9], and Fetrati and Pak [10] used FEM approach for prediction of sand production. Ghassemi and Pak [11], Li et al. [12], and Seyed Atashi et al. [13] used DEM approach for simulating sand production.

For overcoming the limitation of the discrete element method; in this study, the continuum approach is used for simulation of sanding problem. This paper examines the utility of a coupled hydromechanical and erosion criterion for simulating sand production based on the finite element method. For simulating erosion, a number of sand erosion criteria proposed by various researchers were selected and implemented into the finite element code. Erosion equations are defined using Umeshmotion subroutine written in Fortran and linked to Abaqus. Erosion equations consider both plastic strain in the rock, and fluid flow velocity which are effective parameters in sanding phenomenon.

In the FEM context, it is well-known that the more mesh is distorted, the less accuracy is obtained in the numerical simulation. Given that the sand production phenomenon leads to significant deformation near the wellbore, it is vital that keep the mesh quality high. According to the importance of mesh quality; in this study, Arbitrary Lagrangian-Eulerian (ALE) adaptive meshing technique is used which makes it possible to maintain a high-quality mesh throughout sand production procedure, even when large deformation occurs, by allowing the mesh to move independently of the material.

Another technique that may be needed for simulation of sanding is Map solution. The solution mapping technique is used when elements become so severely distorted during an analysis that they no longer provide a proper discretization of the problem. Map solution technique maps the solution from an old, deformed mesh to a new mesh so that the analysis can continue, and it can be used only with continuum elements. For using this technique, it is needed to use Python code in Abaqus.

This paper is organized as follows. In Sec. 2, the basic theory is explained. In Sec. 3, the laboratory experiments and numerical modeling procedures are described, and numerical results are compared with the experimental results. Sec. 4 and Sec. 5 are dedicated to parametric study and conclusions, respectively.

2. MODEL THEORY

2.1. Material Constitutive Model

The sand production process is generally related to two important mechanisms: 1) the mechanical failure of the rock around the wellbore, and 2) hydro-mechanical instability from internal and surface erosion due to fluid drag forces or seepage forces resulting in the dislodgement and migration of loose particles [9]. So, an elasto-plastic constitutive behavior of the rock should be considered when a continuum-based approach is of concern. The Mohr-Coulomb model associated with a hardening/softening scheme is used in this study. For general states of stress, the model is conveniently written in terms of the stress invariants as:

$$F = R_{mc} q - p' \tan\phi - c = 0 \qquad 1$$

where

$$R_{mc}(\theta,\phi)=\frac{1}{\sqrt{3}\cos\phi}\sin(\phi+\frac{\pi}{3})+\frac{1}{3}\cos(\theta+\frac{\pi}{3})\tan\phi \quad 2$$

ϕ is the friction angle of the material, c is the cohesion of the material, p' is the equivalent pressure stress, q is the Mises equivalent stress, θ is the deviatoric polar angle defined as

$$\cos(3\theta)=(\frac{r}{q})^3 \quad 3$$

and r is the third invariant of deviatoric stress.

$$r=(\frac{9}{2}S.S:S)^{1/3} \quad 4$$

$$q=\sqrt{\frac{3}{2}(S:S)} \quad 5$$

where S is the deviatoric stress

$$S=\sigma+pI \quad 6$$

It has been shown that for ameliorating the accuracy of sand production modeling, an elastic-perfect-plastic model is not sufficient and a hardening/softening scheme should be incorporated. The sand must enter a strain softening regime before it can be disaggregated [14]. For considering the softening behavior of rock; in this paper, the cohesion degeneration is reflected by defining a mobilized cohesion as a function of plastic strain [15].

$$\bar{C}=C_0\exp\left[-\left(\frac{\bar{e}_p}{e_e^c}\right)\right] \quad 7$$

where $\bar{C}$ is the mobilized cohesion; C_0 is initial cohesion; $\bar{e}_p$ is plastic strain during the softening process and e_e^c is plastic strain which above a certain value of that, assumed the rock disintegrating will be happened. The parameters $\bar{e}_p$ and e_e^c are directly reported in the experiment or obtained through calibrations with laboratory results.

Finally, the severity of the damage of the rock around the wellbore or perforations is evaluated by considering the intensity and the distribution of the equivalent plastic strain

$$\bar{\varepsilon}^{pl}=\int\frac{1}{c}\underline{\underline{\sigma}}:d\varepsilon^{pl} \quad 8$$

where $\underline{\underline{\sigma}}$ is the stress tensor, c is the cohesion, $d\varepsilon^{pl}$ is the plastic strain increment.

2.2. Sanding Criteria

As was mentioned in the previous section, sanding criteria along with the constitutive material model are required for considering the erosion of material near the wellbore or perforations. In this paper, two sanding criteria are used. The sanding erosion equation 9 and 10 were proposed by Papamichos and Stavropoulou [16], and Papamichos and Malmanger [17], respectively.

$$\frac{\dot{m}}{\rho_s} = \lambda c(1-\varphi)\|q_i\| \qquad \lambda(\bar{\varepsilon}^{pl}) = \begin{cases} 0 & if\ (\bar{\varepsilon}^{pl} < \bar{\varepsilon}_{cr}^{pl}) \\ \lambda_1(\bar{\varepsilon}^{pl} - \bar{\varepsilon}_{cr}^{pl})\ if\ (\bar{\varepsilon}^{pl} > \bar{\varepsilon}_{cr}^{pl}) \\ \lambda_2 & if\ \lambda_1(\bar{\varepsilon}^{pl} - \bar{\varepsilon}_{cr}^{pl}) > \lambda_2 \end{cases} \qquad 9$$

$$\frac{\dot{m}}{\rho_s} = \lambda c(1-\varphi)\|q_i\| \qquad \lambda(\bar{\varepsilon}^{pl}) = \begin{cases} 0 & if\ (\bar{\varepsilon}^{pl} < \bar{\varepsilon}_{cr}^{pl}) \\ \lambda_1(\bar{\varepsilon}^{pl} - \bar{\varepsilon}_{cr}^{pl})\ if\ (\bar{\varepsilon}_{cr}^{pl} \le \bar{\varepsilon}^{pl} \le \bar{\varepsilon}_{cr}^{pl} + \lambda_2/\lambda_1) \\ \lambda_2 & if\ \bar{\varepsilon}^{pl} > \bar{\varepsilon}_{cr}^{pl} + \lambda_2/\lambda_1 \end{cases} \qquad 10$$

where $\dot{m}$ is the erosion rate of solid mass, c is the transport concentration of the fluidized solids, ρ_s is the solid density, φ is the porosity, q_i is the fluid flux and the symbol $\|\ \|$ is the norm of the function that only assigns positive values of q_i, λ is the sand production coefficient, $\bar{\varepsilon}_{cr}^{pl}$ is the critical plastic shear strain at peak strength, and $\lambda_1$and λ_2 are calibration constants which can be obtained through calibrations with experimental sand production data.

The applicability of equation 9 was examined for an oil field located in the North Sea [10]. In this study, the applicability of the sand erosion models is investigated for two laboratory experiments, and the results are compared with experimental records. Sand production in a horizontal wellbore and a perforated casing completion were tested in the laboratory as explained in Sec. 3.1 and Sec. 3.2, respectively.

3. LABORATORY EXPERIMENTS AND NUMERICAL SIMULATION

3.1. Sand Production in Horizontal Wellbore

This experiment was conducted on a low-strength artificial sandstone block (26.25 cm×26.25 cm×38 cm) with a 25.4 mm diameter horizontal hole. The purpose of the experiment was examination of the behavior of horizontal wellbores, and the amount of producing sand under various load conditions [18].

Due to symmetry, only one-quarter of the model was considered in the numerical modeling. In the analysis, the initial conditions, both stresses and pore pressures, were set to zero, and plane strain condition was assumed for simulation. Afterward, stresses were gradually increased following the experimental procedure.

The geometry of the model used in the numerical modeling is shown in Figure 2**, and the magnitude of the applied vertical stress on the top boundary and the variations of the flow rate which applied to the right and top boundaries, are shown in** Figure 1**. Throughout the simulation, the pressure inside the central hole was set to atmospheric pressure. Also, the ratio between vertical and horizontal effective stresses was kept at a fixed value of 2. Physical and mechanical properties that used in the numerical and experimental simulation are shown in** Table 1.

The deformation and pore pressure were primary unknown variables during the simulations. Therefore, the coupled deformation and pore pressure element CPE4P in Abaqus was used, which is a 4-node bilinear displacement and pore pressure element. Equation 9 was

exercised for simulating erosion in this experiment.

During the simulation, due to the weak nature of the sandstone used in this experiment, deformation near the wellbore was very large. Consequently, in addition of ALE technique, Map solution technique was used for avoiding severe element distortion.

The obtained numerical results are compared with the experimental data and the result of other numerical simulations by Pak et al. [5] and Nouri et al. [6] in Figure 4. The obtained results not only qualitatively agree with the experimental results; it also matches well with the experimental recordings.

Figure 3 shows the velocity profile on the wellbore surface at different times. It can be seen that at early production time (9600s and 15500s) the fluid velocity around the wellbore is relatively uniform. However, as the eroded area develops unevenly around the wellbore, the fluctuation of fluid flux is escalated.

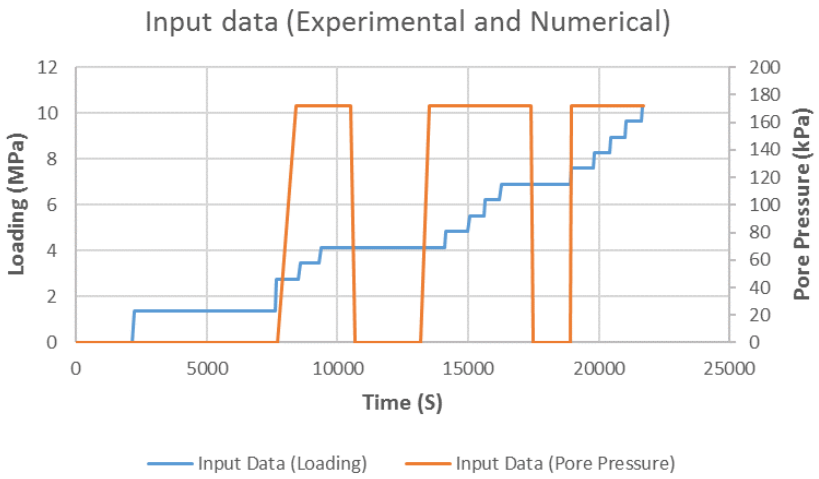

Figure 1. Vertical top boundary stress and flow rate

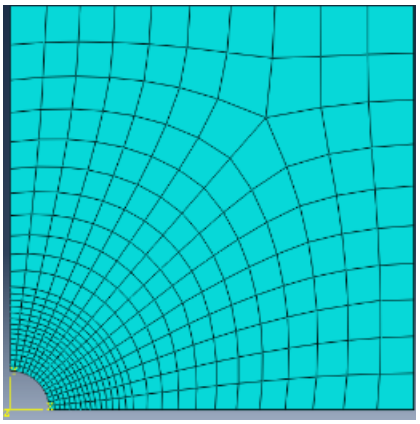

Figure 2. Finite element mesh

Table 1. Input parameters

Parameter	Magnitude	Unit	Parameter	Magnitude	Unit
Young's modulus [GPa]	0.4	GPa	Final cohesion	460	kPa
Density	1750	Kg/m^3	DrawDown	172	kPa
Poisson's ratio	0.05	-	Initial pore pressure	0	kPa
Permeability	3000	mD	Fluid density	1000	Kg/m^3
Void ratio	0.5151	-	Sand production coefficient (λ_1)	1	1/m
Friction angle	37.5	°	Sand production coefficient (λ_2)	0.075	1/m
Dilation angle	7.5	°	Transport concentration of the fluidized solids	0.001	-
Initial cohesion	1250	kPa	Critical equivalent plastic strain	0.028	-

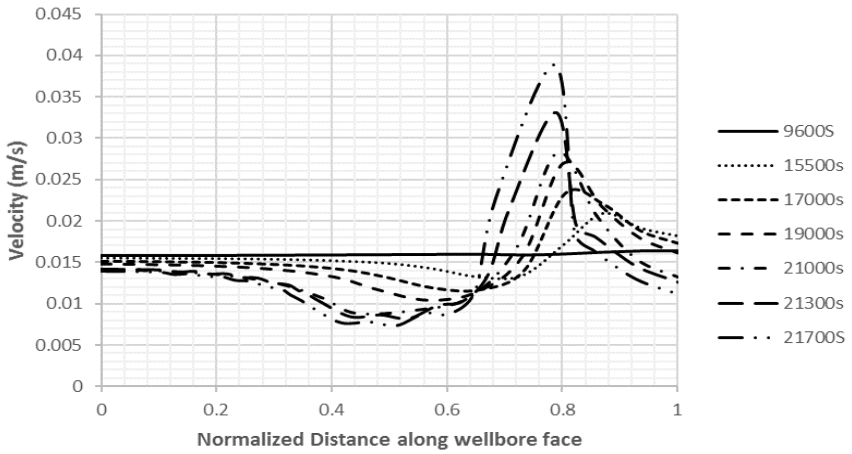

Figure 3. Fluid flow velocity on the wellbore surface at different production times

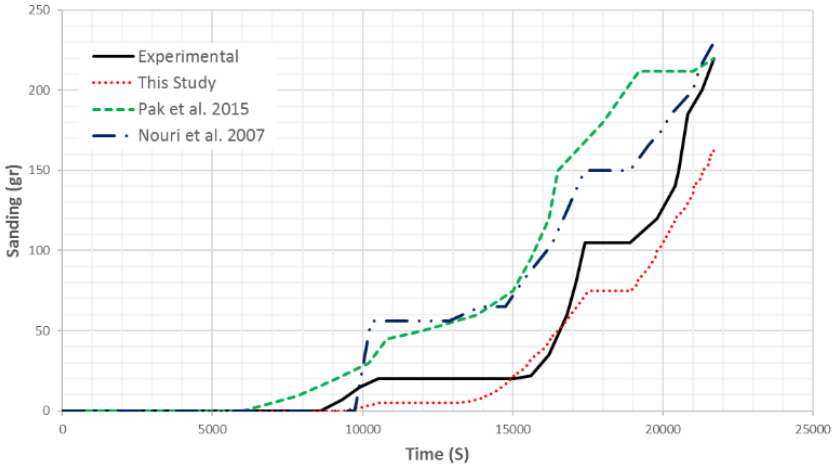

Figure 4. Cumulative sand production

3.2. Simulation of a Real Well with Multiple Perforations

The objective of the experiment [19], which was the first of its kind, was to investigate the influence of both effective stress increase and drawdown on sand production. A sandstone block of 0.7 m×0.7 m×0.81 m was used in this experiment. According to the mineralogy tests, the rock sample composed of 70% quartz and 30% mixed feldspars [19]. The stresses applied in the vertical, and two horizontal directions could vary independently to simulate the required stress state. From a single inlet point, the pore fluid was distributed over the four vertical sides of the block through a wide pore pressure jacket. The flowline through which the fluid was produced started at the bottom of the wellbore and ended in a pair of buckets that contained 230-mesh sand screens, designed to trap the sand (Figure 5).

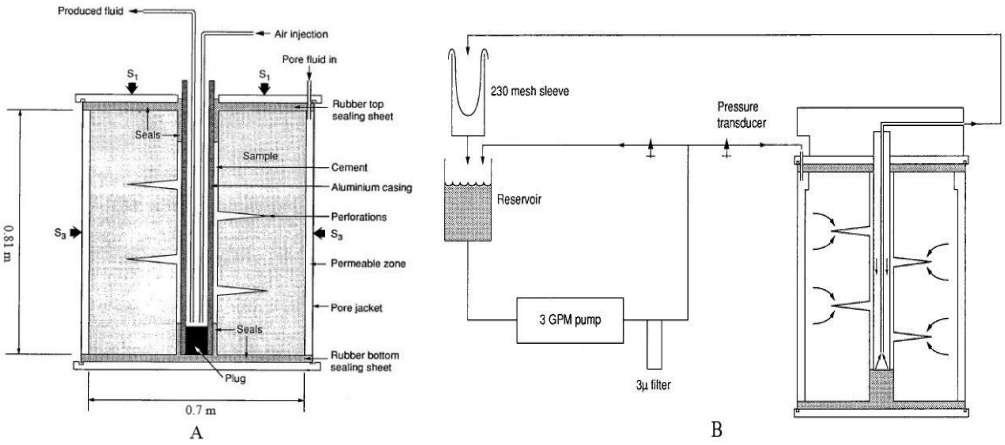

Figure 5. A) Polyaxial cell stress frame; B) Flow/sieve system schematic [19]

In the numerical simulation, axial symmetry was assumed. Fine finite element mesh was set in the model near the perforation (Figure 7). A zero pore pressure was defined in the perforation edge to simulate the atmospheric pressure in the wellbore. Different fluid pressures, horizontal stresses and vertical stresses applied on the block sample as shown in Table 2. Input parameters that used in the numerical simulation are shown in Table 3.

Table 2. Numerical analysis steps

	σ_v (MPa)	σ_h (MPa)	P_P (MPa)	t (hr)
Initial conditions	12.40	6.82	3.44	0
Intermediate	9.30	3.72	0	0.28
DD_A	9.92	4.34	0.689	1.36
DD_B	10.54	4.96	1.38	2.08
DD_C	11.16	5.58	2.07	3.00
DD_{D1}	11.78	6.20	2.76	4.26
DD_{D2}	11.78	6.20	2.41	5.96
DEP_A	17.98	8.68	2.41	7.54
Shut-in	15.81	6.51	0	7.68
Bean-up	17.98	8.68	2.41	8.54
DEP_B	24.18	11.16	2.41	9.36

Table 3. Input parameters

Parameter	Magnitude	Unit	Parameter	Magnitude	Unit
Young's modulus [GPa]	6.8	GPa	Initial cohesion	5	MPa
Density	1900	Kg/m^3	Final cohesion	0.5	MPa
Poisson's ratio	0.178	-	Fluid density	1000	Kg/m^3
Permeability	3600	mD	Sand production coefficient (λ_1)	1.5	1/m
Void ratio	0.35135	-	Sand production coefficient (λ_2)	0.03	1/m
Friction angle	37	°	Transport concentration of the fluidized solids	0.0001	-
Dilation angle	7	°	Critical equivalent plastic strain	0.00325	-

For simulation of the effect of the stiff solid cement and the casing, the displacement of the wellbore surface was constrained, and the lower edge boundary was fixed in the vertical direction (Figure 7). Finally, equation 10 employed for simulation of erosion in this experiment.

The numerical results are compared with the experimental records in Figure 6. A good agreement is observed between the numerical and experimental results. The results show the sanding criterion that used in this experiment can predict the amount of sanding in different circumstances very well.

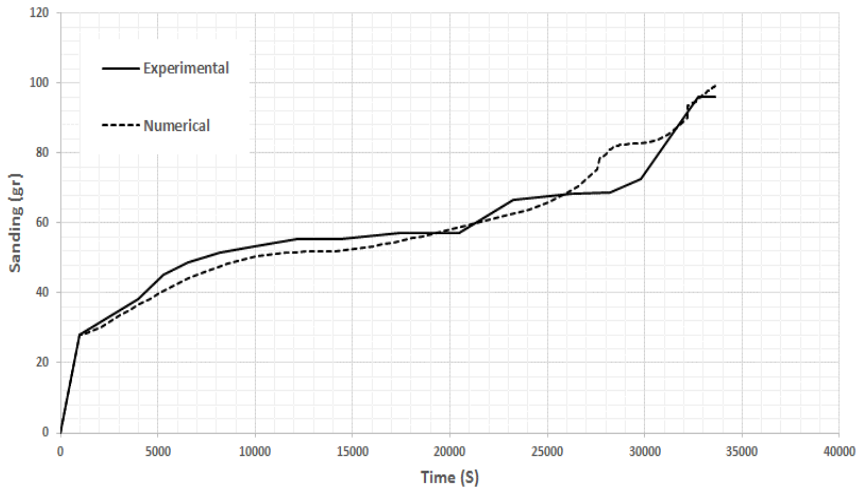

Figure 6. Fluid flow velocity on the wellbore surface at different production times

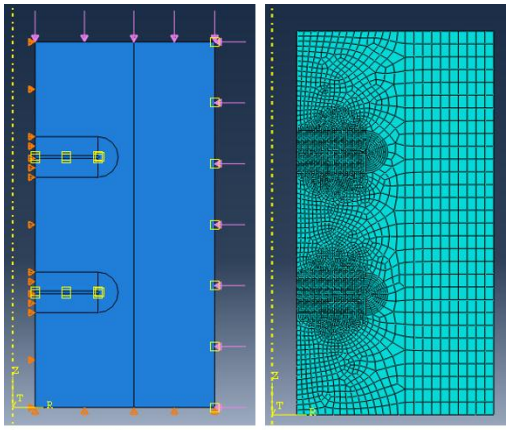

Figure 7. A) Boundary condition; B) Finite element mesh

4. PARAMETRIC STUDY

4.1. Permeability

One of the methods for improving the production of wells is acidizing, which increases the permeability of the well, but beyond that, increase in permeability may increase the magnitude of sanding. Having information about how the permeability can affect the amount of sand production is necessary. Hence, the effect of this parameter is examined in this section. Figure 8 illustrates the effect of permeability coefficient on the sanding. As shown, the amount of sanding is very sensitive to the permeability coefficient.

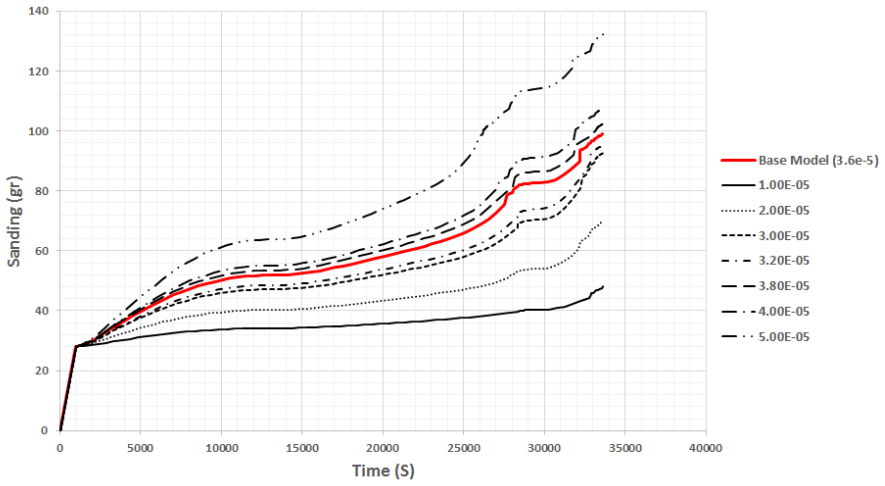

Figure 8. The quantities of sand produced in different permeability

4.2. Friction angle

The friction angle is one of the factors affecting rock strength. Therefore, with lower

friction angle, rock yields faster and leads to increase of sand production. Figure 9 shows the effect of friction angle on the sanding phenomenon.

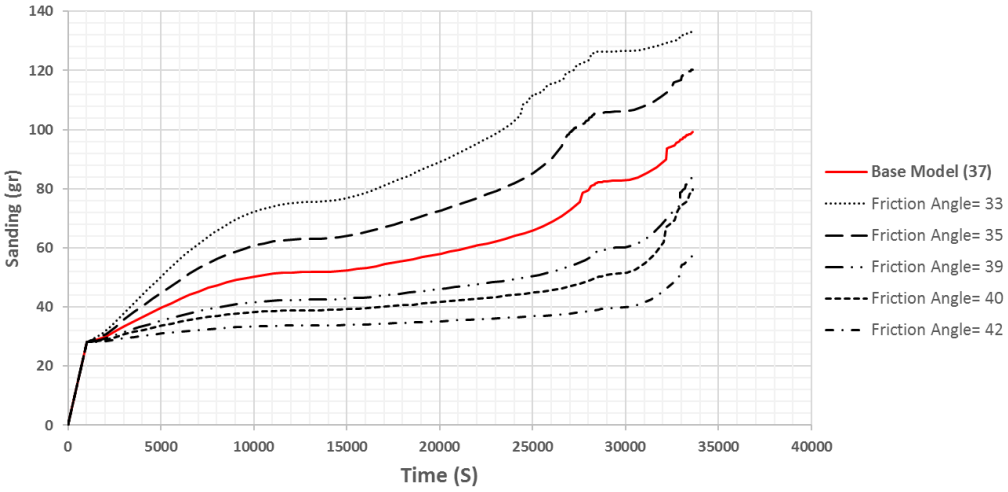

Figure 9. The quantities of sand produced in different friction angle

5. CONCLUSIONS

A hydromechanical sand erosion model along with two sanding criteria for simulation of sand production phenomenon on the wellbores was used in this study. The results of numerical modeling of laboratory experiments and parametric study with Abaqus culminate in:

1. Sanding criteria that incorporate the "plastic shear strain" and "erosion rate" can predict the onset of sanding and sanding amount with a good level of accuracy.
2. Effect of reservoir rock permeability on the sand production is high. Under similar conditions, if the permeability coefficient is increased from 3.6×10^{-5} to 5×10^{-5}, the amount of sanding increases from 100 gr to 130 gr.
3. Effect of friction angle on sanding is also considerable. For each 5° increase in the friction angle, sanding decreases up to 44 percent.

6. REFERENCES

[1] V. Fattahpour, M. Moosavi, and M. Mehranpour, "An experimental investigation on the effect of rock strength and perforation size on sand production," J. Pet. Sci. Eng., vol. 86–87, pp. 172–189, 2012.

[2] M. Dusseault and F. J. Santarelli, "A conceptual model for massive solids production in poorly-consolidated sandstones," ISRM Int. Symp., pp. 789–797, 1989.

[3] H. Rahmati et al., "Review of Sand Production Prediction Models," J. Pet. Eng., vol. 2013, pp. 1–16, 2013.

[4] C. Detournay, "Numerical Modeling of the Slit Mode of Cavity Evolution Associated With Sand Production," SPE J., vol. 14, no. 04, pp. 797–804, 2009.

[5] A. Pak, B. Abbasi, B. Rouhbakhsh, and A. Selseleh, "Numerical Study of Sand Production in Oil Extracting Wells (In Persian)," in 1st National Conference on Petroleum Geomechanics, 2015, pp. 1–9.

[6] A. Nouri, H. Vaziri, H. Belhaj, and M. R. Islam, "Comprehensive transient modeling of sand production in horizontal wellbores," Spe J., vol. 12, no. 4, pp. 468–474, 2007.

[7] S. Bodaghabadi, M. Mousavi, and J. Mousavi, "Sand Production Prediction Using Numerical Method (In Persian)," J. Fac. Eng. (University Tehran), vol. 41, no. 3, pp. 263–271, 2007.

[8] X. Li, Y. Feng, and K. E. Gray, "A hydro-mechanical sand erosion model for sand production simulation," J. Pet. Sci. Eng., vol. 166, pp. 208–224, 2018.

[9] K. Eshiet and Y. Sheng, "Influence of rock failure behaviour on predictions in sand production problems," Environ. Earth Sci., vol. 70, no. 3, pp. 1339–1365, 2013.

[10] M. Fetrati and A. Pak, "Prediction of Sand Production in Oil Wells Using Numerical Simulation (In Persian)," in 3rd Iranian Conference of Geotechnical Engineering, 2018, pp. 1–9.

[11] A. Ghassemi and A. Pak, "Numerical simulation of sand production experiment using a coupled Lattice Boltzmann-Discrete Element Method," J. Pet. Sci. Eng., vol. 135, pp. 218–231, 2015.

[12] L. Li, E. Papamichos, and P. Cerasi, "Investigation of sand production mechanisms using DEM with fluid flow," in Eurock 2006: Multiphysics Coupling and Long Term Behaviour in Rock Mechanics, Taylor & Francis, 2006, pp. 241–247.

[13] S. M. Seyed Atashi, K. Goshtasbi, and R. Basirat, "Fluid Properties Effects on Sand Production using Discrete Element Method," J. Chem. Pet. Eng., vol. 52, no. 2, pp. 171–181, 2018.

[14] A. Nouri, E. Kuru, and H. Vaziri, "Elastoplastic Modelling of Sand Production Using Fracture Energy Regularization Method," J. Can. Pet. Technol., vol. 48, no. 04, pp. 64–71, Apr. 2009.

[15] P. A. Vermeer and R. de Borst, "Non-Associated Plasticity for Soils, Concrete and Rock.," Heron, vol. 29, no. 3, pp. 1–64, 1984.

[16] E. Papamichos and M. Stavropoulou, "An erosion-mechanical model for sand production rate prediction," Int. J. Rock Mech. Min. Sci., vol. 35, no. 4–5, pp. 531–532, 1998.

[17] E. Papamichos, E. M. Malmanger, and S. Petroleum, "A Sand-Erosion Model for Volumetric Sand Predictions in a North Sea Reservoir," Engineering, no. July 1999, pp. 21–23, 2001.

[18] A. P. Kooijman et al., "Horizontal-Wellbore Stability and Sand Production in Weakly Consolidated Sandstones," SPE Drill. Complet., vol. 15, no. 04, 2000.

[19] A. Kooijman and P. Halleck, "Large-scale laboratory sand production test," 67th Annu. Tech. Conf. Exhib. Soc. Pet. Eng., pp. 325–338, 1992.